Nanoscale Advances

ROYAL SOCIETY OF CHEMISTRY

PAPER

View Article Online
View Journal | View Issue

Cite this: *Nanoscale Adv.*, 2021, **3**, 6739

Tuning the interface in epoxy-based composites and laminates through epoxy grafted graphene oxide enhances mechanical properties

Prajakta Katti, K. K. Verma, S. Kumar* and Suryasarathi Bose *

Improved dispersion together with enhanced interfacial adhesion of the reinforcement is the key to superior structural properties in polymer nanocomposites. Herein, graphene oxide (GO) is employed to reinforce epoxy, and in order to improve the interfacial adhesion, epoxy chains were grafted directly onto GO prior to composite preparation. The functionalized GO sheets were systematically characterized using FTIR, TEM, Raman spectroscopy, XRD, and XPS. The epoxy composites with GO and epoxy grafted graphene oxide (Ep-g-GO) were prepared with the addition of only a small amount (0.5 wt%) of GO using a mechanical stirrer coupled to a bath sonicator. This strategy resulted in an impressive increase in mechanical properties, 40% in storage modulus, 70% in hardness, 39% in fracture toughness, and 8% in tensile strength, as compared to neat epoxy. In addition, the modified composites were thermally stable up to 300 °C as inferred from the thermogravimetric analysis. The enhanced properties of the composites further led to investigating the effect of Ep-g-GO on epoxy/carbon fiber (CF) laminates. Interestingly, incorporation of 0.5 wt% Ep-g-GO resulted in improved interfacial adhesion between GO and the epoxy matrix, which enhanced the tensile strength by 12% and inter-laminar shear strength by 9% as compared to neat epoxy/CF laminates. This study clearly demonstrates the positive effect of the tailored interface, offered by Ep-g-GO, on the mechanical properties of epoxy composites and epoxy/CF laminates.

Received 13th June 2021
Accepted 27th September 2021

DOI: 10.1039/d1na00437a

rsc.li/nanoscale-advances

Introduction

The use of carbon fiber (CF) reinforced polymer matrix laminates has witnessed a substantial growth in various applications such as aerospace and automotive sectors due to their high specific strength and modulus, light weight, and their ability to be tailored for a myriad of applications.[1–3] Around 50% of the aircraft structure is made up of CF reinforced laminates. Epoxy is a thermosetting polymer, which is widely used as a matrix in CF reinforced laminates. Epoxy is also widely used in a variety of other applications such as electronics, adhesives, and coatings.[4] The benefits of epoxy over other thermosets have been well documented in the literature. The cured cross-linking structure of epoxy possesses an excellent combination of properties like excellent thermal stability, chemical resistance, mechanical properties, and processability. The main drawback with epoxy is its inherent brittle nature and also poor crack resistance, which restricts its utility in structural applications.[5,6] The physical and mechanical properties of these laminates strongly depend mainly on three factors namely polymer matrix, fiber reinforcement, and interfacial interactions between the two.

The modes of failure in epoxy/CF laminates are delamination within epoxy/CF laminates, debonding between epoxy and CFs, and fracture of CFs. It is well known that the fiber/matrix interface facilitates the stress transfer from the weak matrix to the strong fiber, so the performance of the laminate is largely dependent on the fiber/matrix adhesion.[7–9] Hence, a lot of research is focused on improving their performance predominantly to improve the toughening of epoxy, and the interface between epoxy and CFs.[10,11] Various thermoplastics like polyethersulfone (PES), polysulfone (PSF), poly(aryl ether ketone), polyimides (PI), polyphenyl ether, *etc.* are also being used to toughen the epoxy matrix.[12] But the challenge is their processability and cost. Hence, researchers came up with new strategies like reinforcing epoxy with nanofillers such as carbon nanotubes (CNTs) and graphene oxide (GO), which has gained significant interest of late due to their outstanding properties such as strength, stiffness, and high electrical and thermal conductivity.[13,14] As compared to thermoplastics, incorporation of nanofillers into an epoxy matrix holds promise in delivering exceptional mechanical, thermal, and multi-functional properties at relatively lower filler loading. The advantage of GO over CNTs is that it has abundant functional groups like carboxyl, hydroxyl, and epoxide groups. These GO sheets with sp^2 hybridization are amphiphilic in nature with hydrophilic edges and a hydrophobic basal plane, which facilitates strong

Department of Materials Engineering, Indian Institute of Science, Bangalore-560012, Karnataka, India. E-mail: skumar@iisc.ac.in; sbose@iisc.ac.in

interaction with both polar and nonpolar polymers.[15–17] However, the challenge with GO sheets is that it has a high tendency to form agglomerates due to the van der Waals' forces and strong π–π stacking.[4,18] Nevertheless, the abundant functional groups facilitate the conjugation of GO with the polymer matrix, which in turn results in better dispersion of GO sheets.

In the present study, an attempt has been made to improve the mechanical properties of epoxy by incorporating GO sheets. The novelty of the present work is that the epoxy chains were grafted onto GO sheets by a chemical route before they were incorporated into the epoxy matrix. As the grafted epoxy chains are compatible with the host epoxy, this strategy tailors the GO dispersion in the epoxy and facilitates improved interfacial adhesion with the host epoxy. It is envisaged that this strategy may help in improving the mechanical properties of the epoxy to a great extent. The epoxy grafted GO (Ep-g-GO) is thoroughly characterized by Fourier transform infrared spectroscopy (FTIR), transmission electron microscopy (TEM), Raman spectroscopy, thermogravimetric analysis (TGA), X-ray diffraction (XRD), and X-ray photon scattering (XPS). In addition, the effect of Ep-g-GO on the mechanical and thermal properties of epoxy/CF laminates is also investigated in this study. The laminates were prepared using a vacuum-assisted resin transfer molding (VARTM) process using a GO and Ep-g-GO dispersion and the mechanical properties were compared against control epoxy/CF laminates.

Experimental

Materials

A bisphenol A-epichlorohydrin based epoxy resin (EPOLAM 2063, $M_n \leq 700$) and anhydride-based hardener (1,2,3,6-tetrahydromethyl methanophthalic anhydride) were purchased from Axson Technologies, France. Graphite flakes were procured from Sigma. Ethanol, dimethylformamide (DMF), and triphenyl phosphene were procured from a commercial source and were used without any pre-treatment. The bidirectional CF mats (Hinfab HCP 200A) were procured from Hindoostan Technical Fabrics.

Synthesis of graphene oxide (GO)

GO was prepared by a modified Hummers' method as discussed in our previous study.[19] Graphite flakes were introduced into a mixture of concentrated H_2SO_4 and H_3PO_4 (9 : 1 ratio) in a water bath.[20,21] $KMnO_4$ was then added to the mixture subsequently and the mixture was stirred at room temperature in a closed reactor for 24 h. After completion of the reaction, the mixture was poured into deionized (DI) water and stirred again for 2 h. Then dropwise 35% hydrogen peroxide (~5–10 ml) solution was added to the solution until the color of the solution turned into bright yellow. The solution was then thoroughly filtered, and the filtrate was then washed with DI water, HCl, and ethanol, which was followed by drying in a vacuum oven.

Grafting of epoxy onto GO (Ep-g-GO)

To graft epoxy chains onto GO, 10 g of epoxy resin (Epolam 2063) was dissolved in 50 ml of DMF on a magnetic stirrer for 2 h. Simultaneously, 500 mg of GO was dispersed in 50 ml DMF with the help of bath sonication. Finally, to catalyze the reaction, TPP (0.5 wt% to epoxy) was added into the solution of epoxy and GO in DMF. The solution was kept at 100 °C for 24 h. After completion of the reaction, the filtrate was washed with acetone and water followed by drying at 50 °C in the vacuum oven. The schematic of grafting of epoxy chains onto GO is shown in Fig. 1.

Fabrication of epoxy composites

The fabrication process of epoxy composites containing GO and Ep-g-GO is shown in Fig. 2. This approach ensures homogeneous dispersion of GO and Ep-g-GO in epoxy during the preparation of the composites. Two compositions of epoxy, the first with the addition of 0.5 wt% GO and the second with 0.5 wt% Ep-g-GO, were prepared and the results were compared with those of the neat epoxy. The grafting of epoxy chains onto the GO sheets was analyzed using TGA and the concentration of GO was adjusted accordingly. First, 0.5 wt% GO or Ep-g-GO was dispersed in ethanol and sonicated for 30 min. Then epoxy resin was added and the resultant solution was again bath sonicated for 30 min. The solvent was evaporated from the solution, and the mixture was stirred and

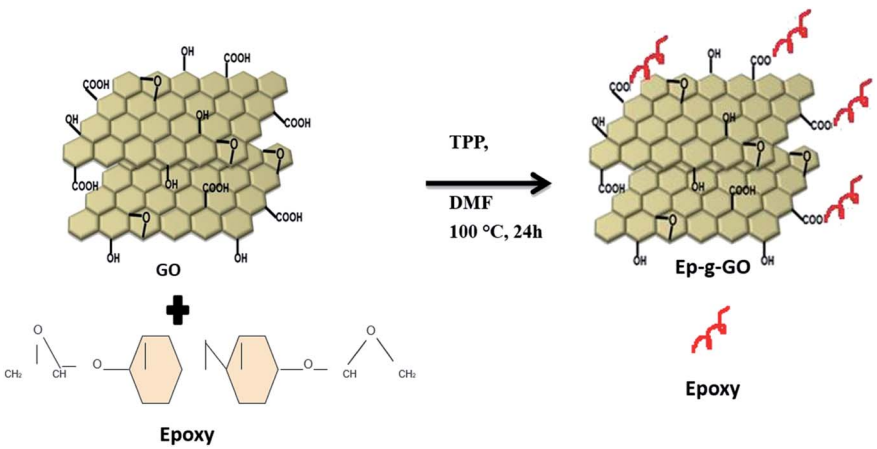

Fig. 1 Synthesis of epoxy grafted GO.

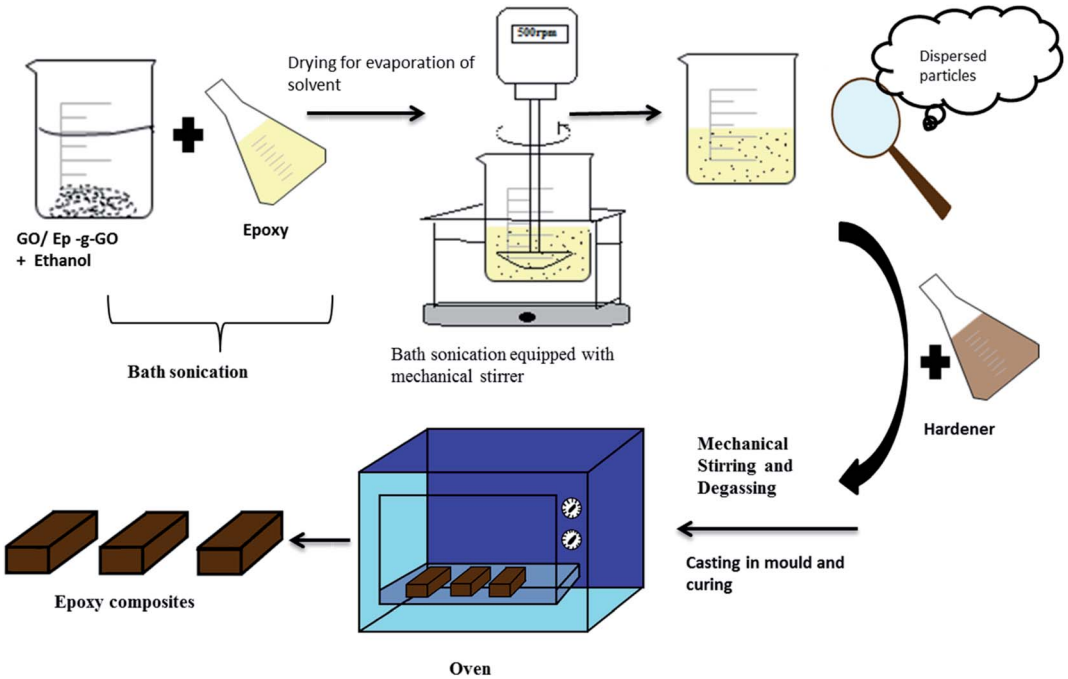

Fig. 2 Schematic of the fabrication process of epoxy/CF composites.

mixed mechanically at 400 rpm using an overhead stirrer coupled to a bath sonicator at 60 °C for 2 h. The hardener was then added in a 100 : 107 ratio followed by 15 min of mixing at 500 rpm. This homogeneously mixed solution was poured in a Teflon coated aluminium mold and cured at 80 °C for 6 h followed by post-curing at 180 °C for 4 h. The samples for different experiments were fabricated according to the American Society for Testing and Materials (ASTM) standards.

Fabrication of epoxy/CF laminates

The epoxy/CF laminate was prepared using the VARTM process. In this process, the reinforcement, that is, bidirectional CF mats, was placed one over the other on a glass plate tool and was infused with epoxy resin under a differential pressure. Fig. 3 illustrates the VARTM process schematically. Eight layers of 300 mm × 300 mm sized carbon mat m were cut systematically. The glass plate was cleaned first, and a release film was placed on the plate. A release fabric (peel ply) was placed over the release film. The CF mats were placed over it in a $[0/90]_8$ lay-up sequence. A release fabric was then placed on top, and the porous release film was placed above it. The release fabric gives a rough texture on the surface, which facilitates the tab bonding on the specimens for tensile testing. A highly permeable resin distribution medium was placed on top for infusion of epoxy with or without GO/Ep-g-GO and the edges were sealed. The entire setup was vacuum bagged. The resin feed was lined on one side and vacuum on the diagonally opposite side. This resin mixture was then preheated to 45 °C and degassed for 20 min to avoid bubbles. The VARTM set-up was also heated in the oven for 30 min at 50 °C. The resin and set-up were preheated in order to keep the resin viscosity during low infusion to ensure the complete wetting of fibers in the CF mat. The viscosity of a resin mixture at 45 °C is 250 cPs. The resin mixture was then infused under a differential pressure followed by curing at 80 °C for 7 h. Post-curing was carried out at 180 °C for 4 h. The specimens were cut using a diamond cutter machine.

Characterization

The as-synthesized GO and Ep-g-GO were analysed by FTIR spectroscopy using a Perkin-Elmer GX in the range of 4000–400 cm^{-1}. The grafting of epoxy onto GO sheets was further confirmed by TEM using an FEI Tecnai T20 S-TWIN, XRD, XPS spectra using a Kratos Analytical instrument with an Al monochromatic source (1.486 keV), and Raman spectra using a LabRAM HR (UV) system with 532 nm laser excitation. Thermal degradation studies and grafting measurements were carried out using a TGA Q500 from TA Instruments, in the temperature range of 30–900 °C in the presence of a nitrogen atmosphere. The dispersion of GO and Ep-g-GO in the epoxy composites was observed by TEM. For TEM analysis of the epoxy composites, about 70 nm sections were trimmed using a Leica Ultramicrotome at room temperature. The fractured morphology behavior of the tensile specimens of the epoxy/CF laminates was evaluated by scanning electron microscopy (SEM) on an ULTRA 55 FESEM (Carl Zeiss). The thermal transition in epoxy composites was observed by Modulated Differential Scanning Calorimetry (MDSC) measurements, which were conducted on a DSC-Q2000 from TA Instruments. The samples were heated at a rate of 2 °C min^{-1} to 200 °C with an amplitude of 1 °C and a period of 60 s. The dynamic mechanical thermal response was studied using a TA Q800 Dynamic Mechanical Analyser (DMA) from TA Instruments. Mode I fracture toughness (K_{1C}) of epoxy composites was determined using a Zwick/Roell screw-driven universal testing machine according to ASTM-D5045-99. Fracture toughness analysis was done at

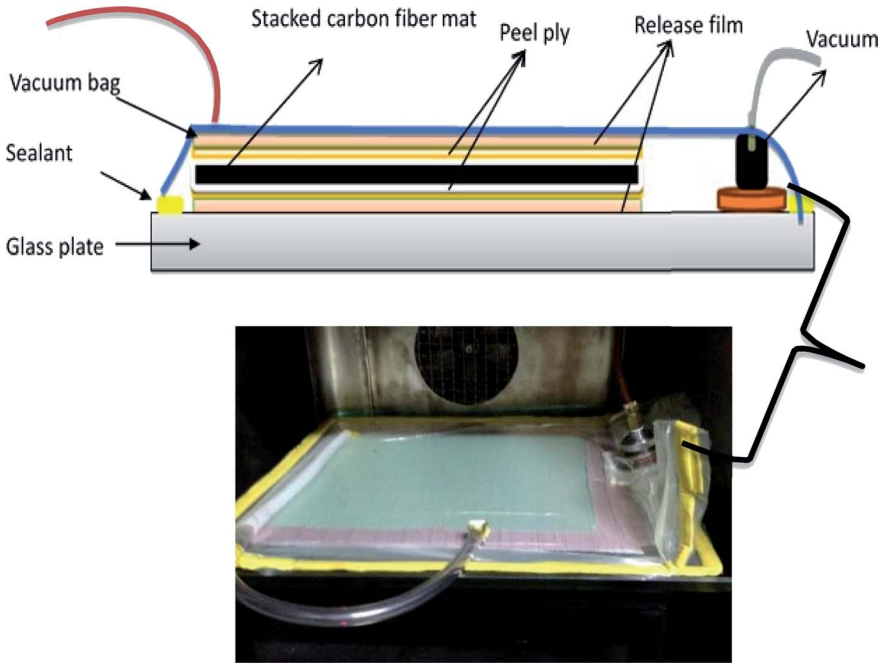

Fig. 3 VARTM process for epoxy/CF laminate preparation.

a crosshead speed of 0.017 mm s^{-1}. The tensile tests of the epoxy composites were carried out on a universal testing machine (Instron 5567) at room temperature according to ASTM-D638. The tensile test of epoxy/CF laminates was carried out as per ASTM-D-3039. The interlaminar shear strength (ILSS) test was carried out as per ASTM-D-2344. The test fixture consisted of a cylindrical roller of 6.0 mm diameter for loading and of 3.4 mm diameter for the side support. Specimens were tested at a cross-head velocity of 0.017 mm s^{-1}. The specimen size was 20 mm × 10 mm × 2 mm. Limiting oxygen index (LOI) tests were carried out as per ASTM-D-2863 using an apparatus from Concept Equipment Ltd, UK. The sample was mounted on a holder and ignited with the burner such that only the upper face was exposed to the flame. The electromagnetic interference (EMI) shielding properties of the epoxy/CF laminates were studied in the Ku-band (12–18 GHz) frequency range using an Anritsu MS4642A vector network analyzer (VNA) using a Keycom waveguide.

Result and discussion

Characterization of GO and epoxy grafted GO (Ep-g-GO)

The grafting of epoxy chains onto GO is confirmed by FTIR, TEM, XRD, Raman spectra, and TGA. Fig. 4 shows the FTIR spectra of GO, epoxy, and Ep-g-GO. The carboxyl group on GO is utilized to harness epoxy chains. In the spectrum of GO, the broad peak centered around 3200 cm^{-1} confirms the presence of hydroxyl groups on the basal plane of GO sheets. The peaks for C–H stretching are observed at 2925 cm^{-1} and 2850 cm^{-1}. The prominent peaks at 1050 cm^{-1} and 1726 cm^{-1} corresponding to epoxy and carboxyl groups, respectively, are also well inferred.[22,23] The existence of these oxygen-containing functional groups further provides evidence of the formation of GO from graphite. The absorption peak in the Ep-g-GO spectrum at 1733 cm^{-1} corresponds to C–O stretching.[24] Absorption peaks at 1624, 1510, 1227, 1036, and 831 cm^{-1} correspond to the absorption of the benzene ring and ether groups of epoxy, which reveals that epoxy chains are grafted onto GO sheets.[25]

The microstructure of GO and Ep-g-GO was further examined using TEM. The TEM images of GO and Ep-g-GO are shown in Fig. 5. The TEM image of GO reveals a thin transparent wrinkled microstructure. However, the TEM image of Ep-g-GO appears darker manifesting a thin layer of epoxy confirming the successful grafting of the epoxy chain onto the GO sheet. The TEM images of epoxy composites with 0.5 wt% GO and 0.5 wt% Ep-g-GO are shown in Fig. 5(c) and (d), and it is

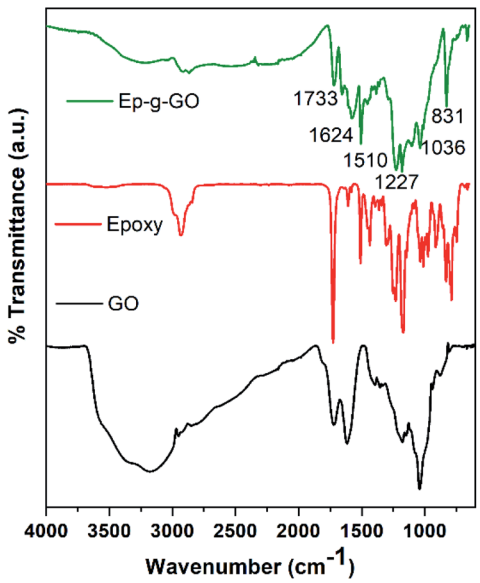

Fig. 4 FTIR spectra of GO, epoxy, and Ep-g-GO.

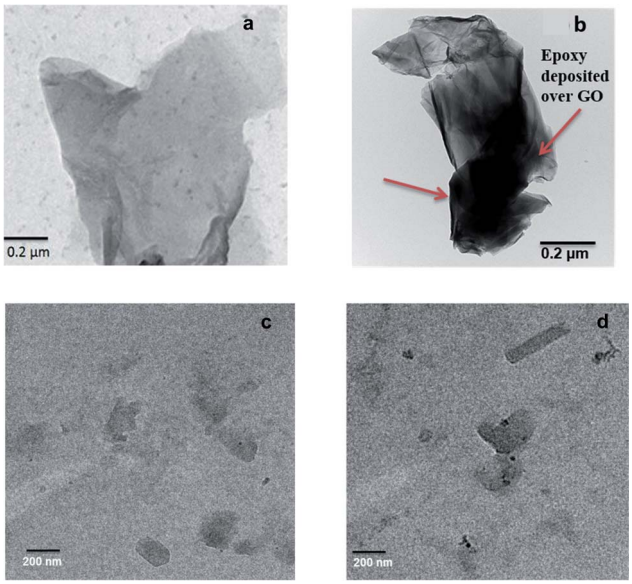

Fig. 5 TEM images of (a) GO, (b) Ep-g-GO, (c) epoxy composite containing GO, and (d) epoxy composite containing Ep-g-GO.

observed that GO and Ep-g-GO are well dispersed in the epoxy matrix. The uniform dispersion of these nanofillers might translate into improved mechanical properties, which will be discussed in the subsequent sections.

Raman spectra of GO and Ep-g-GO are shown in Fig. 6. After the grafting of GO with epoxy, it is observed that the G band for Ep-g-GO shifts from 1593 cm^{-1} to 1586 cm^{-1} indicating the restoration of the sp^2 structure of the graphitic network.[26] It is noticed that the $I_{(D/G)}$ ratio is slightly increased as compared to GO, which is probably due to the reduction in the average size of the in-plane sp^2 domain upon functionalization.

The XRD patterns for GO and Ep-g-GO are shown in Fig. 7. GO flakes exhibit a diffraction peak at 10.9°. The absence of this peak in the case of Ep-g-GO and the appearance of a new broad peak around 18.6° confirms the partial reduction of GO and re-

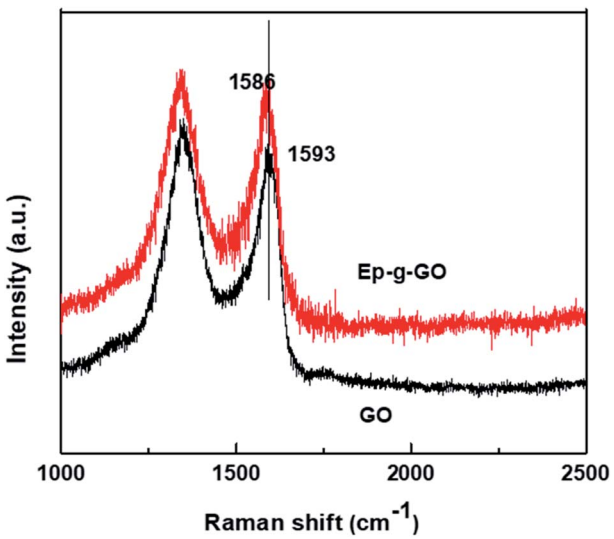

Fig. 6 Raman spectra of GO and Ep-g-GO.

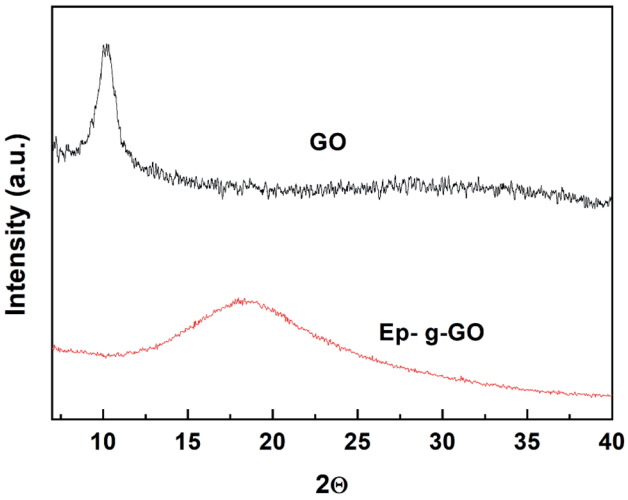

Fig. 7 XRD patterns of GO and Ep-g-GO.

stacking of the sheets. This is due to grafting with epoxy chains, which corroborates the Raman analysis.

The degradation behavior of GO and Ep-g-GO was studied using TGA and is shown in Fig. 8. The TGA of GO shows three-step degradation profiles. The first step is attributed to vaporization of the hydroxyl group (<100 °C); the second step is attributed to the loss of carbonyl group as CO or CO_2 at 150 °C and 200–250 °C, and the final step corresponds to the decomposition of the main graphene chain.[18] The TGA of Ep-g-GO shows mainly one-step degradation around 250 °C accounting for the grafted epoxy chains. However, some minor losses at <100 °C accounting for –OH group pyrolysis and at around 200 °C for the pyrolysis of –COOH groups are observed. The grafting is estimated to be around 30%.

DMA of epoxy and epoxy composites

DMA was carried out to study the viscoelastic behavior of epoxy and epoxy composites. Fig. 9 shows the storage modulus and

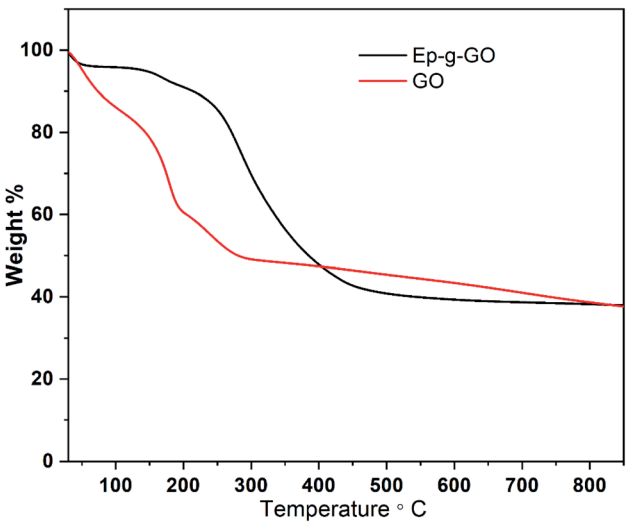

Fig. 8 TGA graphs of GO and Ep-g-GO.

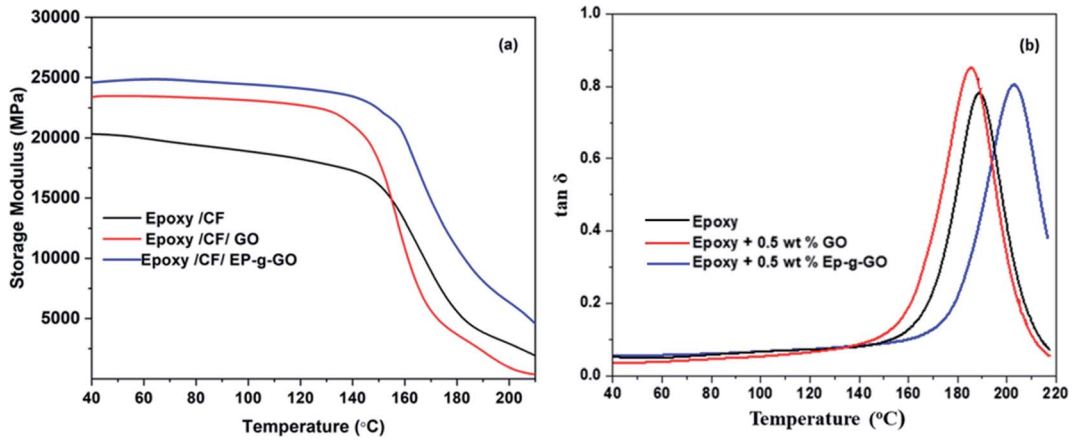

Fig. 9 (a) Storage modulus and (b) tan δ of epoxy and epoxy composites.

Table 1 Mechanical properties of epoxy and epoxy composites

Epoxy/composites	Storage modulus (MPa)	Fracture toughness ($MPa\sqrt{m}$)	Hardness (GPa)	Ultimate tensile strength (MPa)
Epoxy	2700 ± 135	0.77 ± 0.11	0.20 ± 0.01	61 ± 5
Epoxy + 0.5 wt% GO	3500 ± 90	0.92 ± 0.09	0.24 ± 0.05	63 ± 2
Epoxy + 0.5 wt% Ep-g-GO	3779 ± 105	1.07 ± 0.14	0.34 ± 0.03	66 ± 4

tan δ graphs of epoxy and epoxy composites. The addition of 0.5 wt% GO or Ep-g-GO enhanced the storage modulus of epoxy composites by 29% and 40% at 40 °C, respectively, as shown in Fig. 9(a) and Table 1. This improvement in storage modulus is attributed to the reinforcing effects of planar GO sheets, which also result in restricted macromolecular mobility around the sheets. The enhancement in storage modulus is attributed to better dispersion and efficient load transfer from epoxy to GO, which is further improved in Ep-g-GO. In addition, the glass transition temperature (T_g), exhibited by the peak of the curves in Fig. 9(b), of epoxy composites with the addition of GO, was decreased to 185 °C as compared to neat epoxy (188 °C). In contrast, the T_g was enhanced with the addition of Ep-g-GO. The decrease in the T_g for the epoxy composite containing GO is presumably due to hindrance in the cross-linking process on account of abundant functional groups on the basal plane of GO. The enhanced T_g with the addition of Ep-g-GO suggests better dispersion of GO sheets in the epoxy matrix, which may result in restricted chain mobility. In addition, owing to grafting, some of the groups present in GO are utilized and this presumably did not hinder the cross-linking density.

Fracture toughness of epoxy and epoxy composites

The 2D structure together with the abundant functional groups on the surface makes GO a potential candidate to improve the fracture toughness in epoxy composites. A three-point bend test was performed to study the toughening behavior in epoxy. Mode I fracture toughness (K_{IC}) was calculated using the following equations:

$$K_{IC} = \frac{P_q}{\sqrt{BW}} f(x) \quad (1)$$

$$f(x) = 6x^{1/2} \frac{[1.99 - x(1-x)(2.15 - 3.93x + 2.7x^2)]}{(1-2x)(1-x)^{3/2}} \quad (2)$$

where $x=a/W$, P_q = load at fracture, B = specimen thickness, W = specimen width, and a = crack length. The drawback of epoxy is mainly low fracture toughness. However, with the addition of GO and Ep-g-GO, a significant improvement in fracture toughness was observed. It is observed that the enhancement in the fracture toughness of epoxy composites is 19% and 39% with the addition of 0.5 wt% GO and Ep-g-GO, respectively, as shown in Table 1. The rigid GO sheets resist the crack propagation and hence enhance the fracture toughness of the composites. The addition of Ep-g-GO aids in improved dispersion and promotes physical compatibility with the matrix thereby absorbing higher energy and resulting in further enhancement in fracture toughness.[27]

Hardness of epoxy and epoxy composites by nanoindentation

Nanoindentation was carried out using a Berkovich indentor, which monitors and records the load *versus* displacement of the indenter. In this experiment, the maximum load of 8000 μN was applied. The load was applied for 10 s followed by unloading, as shown in Fig. 10(a). The step of holding the load was done to avoid the influence of creep on the unloading characteristics. The load–displacement curves for epoxy and epoxy composites are shown in Fig. 10(b). The maximum indentation load P_{max} divided by the contact area by indentor A gives the hardness H.[28–30]

$$H = \frac{P_{max}}{A} \quad (3)$$

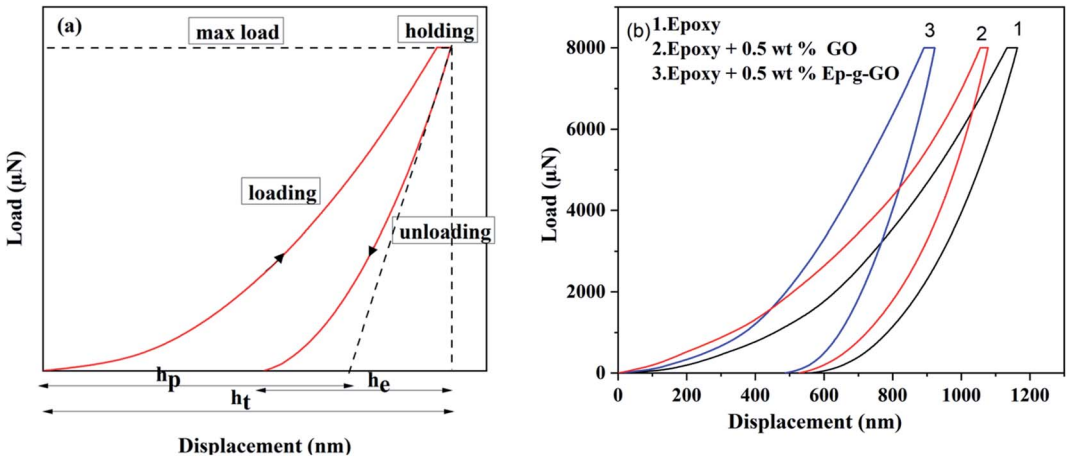

Fig. 10 Representative plots of (a) load as a function of displacement, and (b) load as a function of displacement for epoxy and epoxy composites.

The projected contact area by the Berkovich indentor is calculated from the following equation:

$$A = 24.5 h_p^2 \quad (4)$$

where h_p is the contact indentation depth, as shown in Fig. 10(a).

The hardness values of epoxy and epoxy composites are summarized in Table 1. A significant increment in hardness is observed with the addition of GO and it is further enhanced with the addition of Ep-g-GO. The neat epoxy samples exhibit a hardness of 0.20 GPa, which increases to 0.24 GPa (20%) and 0.34 GPa (70%) with the addition of 0.5 wt% GO and Ep-g-GO, respectively. The enhancement in hardness is attributed to better dispersion and interfacial adhesion of Ep-g-GO with the epoxy matrix.

Tensile properties of epoxy nanocomposites

Fig. 11 illustrates the stress–strain behavior of epoxy and epoxy composites containing GO or Ep-g-GO. It is observed that the ultimate tensile strength (UTS) of epoxy composites improved by about 3% and 8% with the addition of 0.5 wt% GO and Ep-g-GO, respectively. The enhancement in the tensile properties with the incorporation of GO and Ep-g-GO is attributed to the better state of dispersion and interaction of GO and Ep-g-GO with the epoxy matrix, which in turn offers better load transfer at the interface.[4,26,31] Table 1 summarizes the UTS of epoxy and epoxy composites.

Thermal properties of epoxy and epoxy composites by MDSC

The thermal transition in epoxy composites was studied by MDSC. The glass transition temperature (T_g) was then evaluated from the heat capacity plots obtained from the experiment and is displayed in Fig. 12(a). For neat epoxy, the glass transition temperature was observed at around 167 °C and it reduced to 160 °C with the addition of 0.5 wt% GO. Interestingly, the T_g was increased to 174 °C with the incorporation of 0.5 wt% Ep-g-GO. The decrease in T_g with the addition of 0.5 wt% GO is possibly due to the reduced cross-linking density in epoxy.[32,33] Grafting GO sheets with epoxy chains results in increased T_g thereby enhancing the mechanical interlocking of the epoxy chains during the curing process and effectively inhibiting the mobility of epoxy chains.[27,34] A similar trend in T_g of epoxy composites containing GO and Ep-g-GO was observed in DMA as well, which was discussed in the previous section. The thermal stability of epoxy composites was analyzed by TGA. The graphs obtained from TGA are illustrated in Fig. 12(b). It is observed that both the epoxy composites are stable up to 300 °C.

Mechanical and thermal properties of epoxy/CF laminates

From the above results, we observed that GO and Ep-g-GO improve the physical, thermal, and mechanical properties of the epoxy composites. Hence, this strategy of dispersing GO was further extended to improve the properties of epoxy/CF laminates. Epoxy/CF laminates were fabricated as discussed in the Experimental section by the VARTM method.

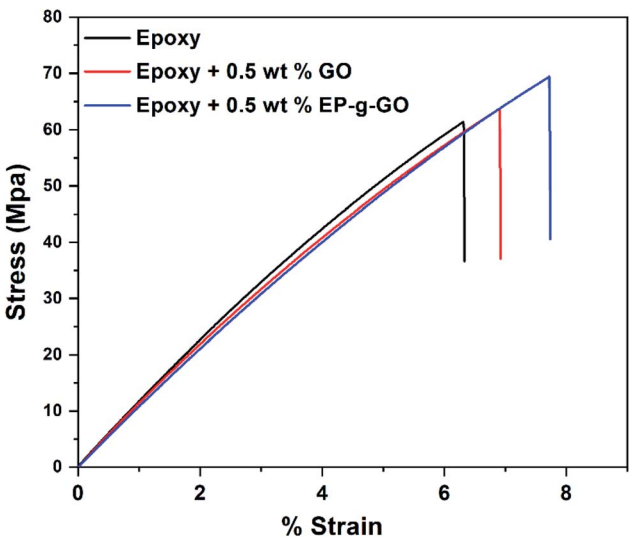

Fig. 11 Stress–strain curves of epoxy and epoxy composites.

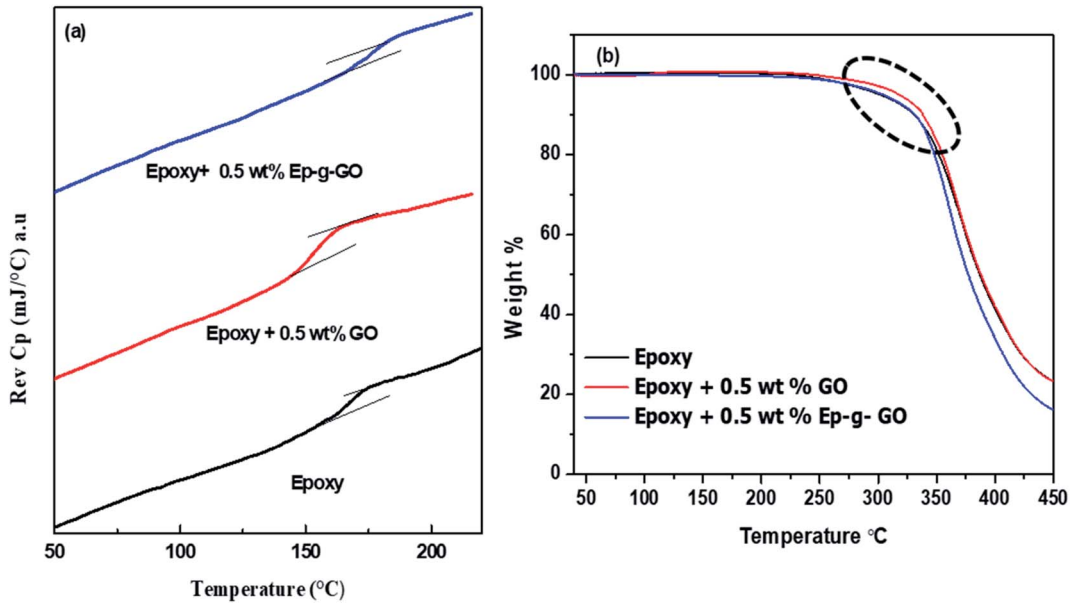

Fig. 12 Thermal analysis of epoxy and epoxy composites by (a) MDSC and (b) TGA.

Fig. 13(a) and (b) show the thermomechanical response of epoxy/CF laminates as a function of temperature. It is observed that for a neat epoxy/CF laminate, the storage modulus at 40 °C was around 20.1 GPa, which increased to 23.3 GPa with the addition of 0.5 wt% GO and further increased to 24.9 GPa with the addition of 0.5 wt% Ep-g-GO in the epoxy matrix. These

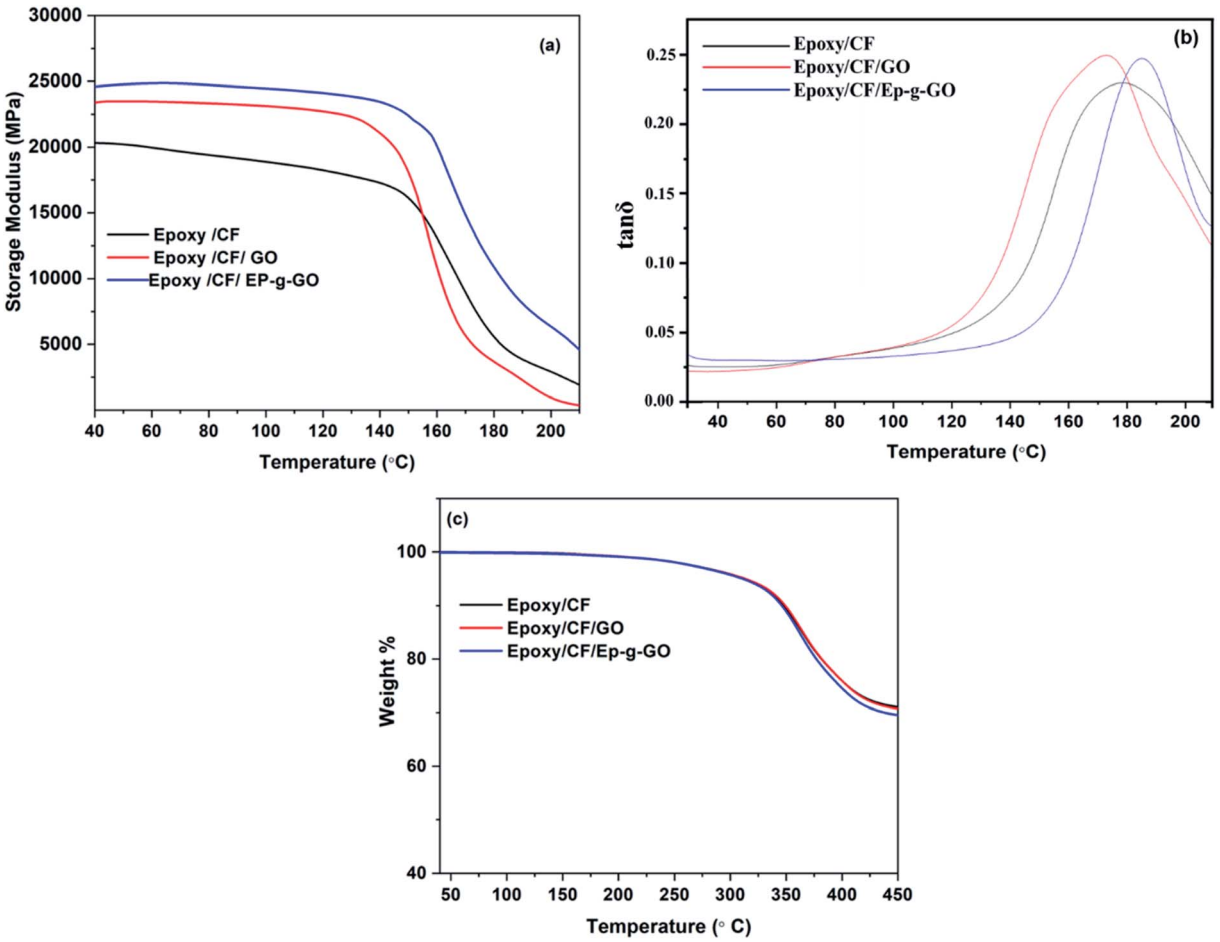

Fig. 13 (a) Storage modulus, (b) tan δ, and (c) TGA graphs of epoxy/CF laminates.

Table 2 Mechanical properties of various epoxy/CF laminates

Laminates	Ultimate tensile strength (UTS) (MPa)	Young's modulus (GPa)	Limiting oxygen index (LOI)	Interlaminar shear strength (ILSS)
Epoxy/CF	733 ± 68	64 ± 2	30	45 ± 2
Epoxy/CF/GO	778 ± 34 (6%)	66 ± 5	31.5	47 ± 2 (4%)
Epoxy/CF/Ep-g-GO	822 ± 14 (12%)	65 ± 2	31.5	49 ± 2 (9%)

nanofillers act as interconnections between the carbon fibers and epoxy and enhance the storage modulus thereby distributing the load by bridging them. The same trend of T_g was observed for epoxy/CF laminates, as was observed in epoxy composites containing GO and Ep-g-GO. The T_g of epoxy/CF laminates decreased with the addition of GO and increased with the addition of Ep-g-GO. From TGA, it was observed that all epoxy/CF laminates were thermally stable up to 300 °C, as shown in Fig. 13(c).

The UTS and Young's modulus deduced from tensile tests are listed in Table 2. The UTS enhanced by about 6% and 12% with the addition of 0.5 wt% GO and Ep-g-GO in epoxy/CF laminates, respectively. The Young's modulus hardly changed with these additions. The ILSS was determined using the following equation.[35]

$$F_{\mathrm{ILSS}} = 0.75 \times \frac{P_{\max}}{b \times h} \tag{5}$$

where F_{ILSS} is the interlaminar shear strength, $P_{\max}$ is the failure load, b is the width of the sample, and h is the thickness of the sample.

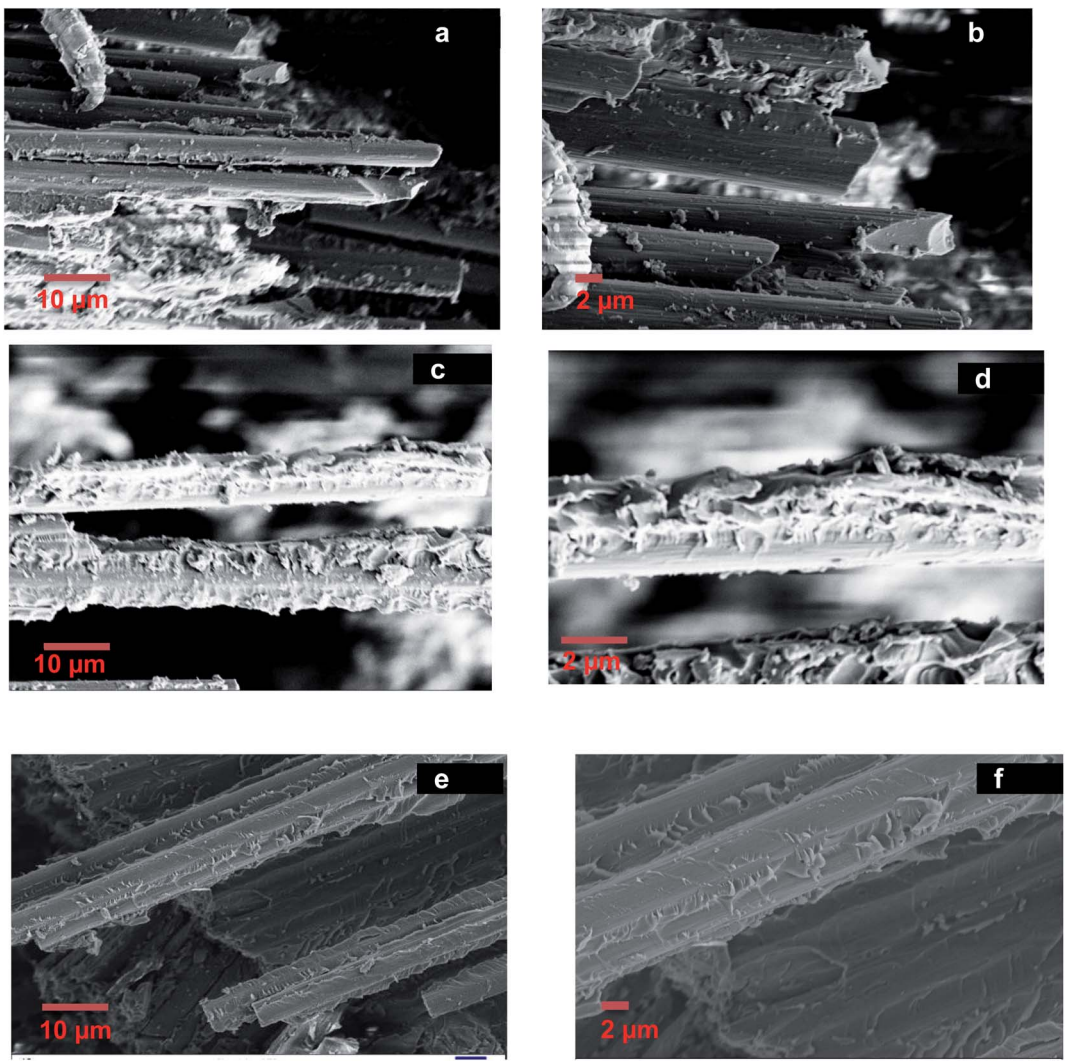

Fig. 14 Fractured SEM images of (a) and (b) epoxy/CF laminates, (c) and (d) epoxy/CF/GO laminates, and (e) and (f) epoxy/CF/Ep-g-GO laminates.

The ILSS values are summarized in Table 2. It is observed that the ILSS properties were improved by 4% and 9% with the addition of 0.5 wt% GO and 0.5 wt% Ep-g-GO, respectively. The SEM fractographs of the failed tensile specimens are shown in Fig. 14(a)–(f). Bare CFs can be observed in epoxy/CF laminates, while a thick layer of epoxy around CFs is observed in epoxy/CF laminates containing GO and Ep-g-GO. The debonding between epoxy and CFs is the dominant failure mechanism in epoxy/CF laminates.

The interaction between the epoxy matrix and carbon fiber interface is responsible for the improvement in the properties and it was observed from SEM images that the epoxy modified with 0.5 wt% Ep-g-GO demonstrated better interfacial adhesion with CF, translating into enhanced mechanical properties.[36,37]

Flammability properties of epoxy/CF laminates

The flame retardancy of polymer samples can be determined by many methods. One of them is by using the LOI, which ultimately gives the flammability behavior of polymeric materials.[38] The flame-retardant properties of the epoxy/CF laminates were analyzed using the LOI. The epoxy resins are highly flammable, with an LOI value of 21.[39]. With the incorporation of the CF mat, the LOI value increased to 30. It is interesting to note that with the addition of GO and Ep-g-GO, the LOI value further increased to 31.5. This indicates that the addition of a small amount of GO and Ep-g-GO can also improve the flammability properties to some extent besides significantly improving the mechanical and thermal properties.[40]

Electromagnetic interference (EMI) shielding

The EMI shielding effectiveness of various epoxy laminates was evaluated in the frequency range of 12 to 18 GHz to explore the possibility of these laminates for applications in EM radiation shielding. The total shielding effectiveness (SE_T) at 18 GHz frequency is shown in Fig. 15. The SE_T can be analyzed using scattering parameters obtained from VNA and is calculated from the following equation[41]

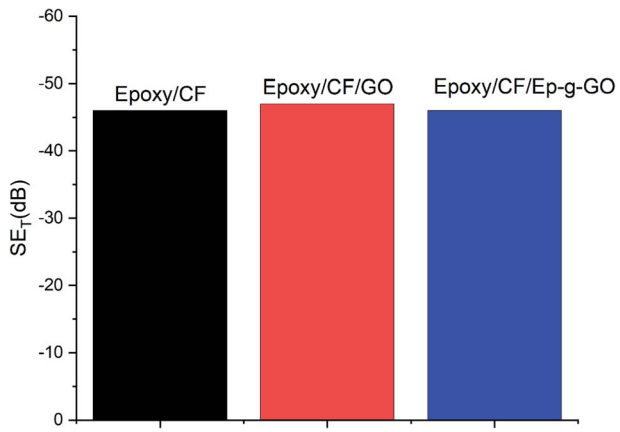

Fig. 15 SE_T of epoxy/CF laminates at 18 GHz.

$$SE_T\ (dB) = 10 \log \frac{1}{|S_{12}|^2} = 10 \log \frac{1}{|S_{21}|^2} \quad (6)$$

where S_{12} and S_{21} are reverse transmission coefficients and forward transmission coefficients, respectively. Two main mechanisms, reflection and absorption, are responsible for EMI shielding. Reflection is enhanced by conductivity and connectivity in the shielding material. The continuous CF mat can act as a wave-guide and can attenuate the incoming EM radiation.[42,43] The continuous CFs present in the matrix play an important role, transporting electrical charges over large distances without electrical losses.[44] The epoxy laminates displayed around −45 dB shielding. It was observed that the modified laminates containing 0.5 wt% GO and 0.5 wt% Ep-g-GO also showed similar shielding effectiveness. This suggests that the charge transfer in the CF mat is essentially unaltered with the incorporation of GO and EP-g-GO. Due to this filler material, there may be the accumulation of charge at the interface, which may result in lossy interfaces. So, these laminates can be used for EMI shielding applications.

Conclusions

In the present investigation, a unique strategy was adopted to improve the dispersion of GO in epoxy composites by covalently grafting epoxy chains onto GO sheets (Ep-g-GO) prior to composite preparation. This strategy has resulted in a 40% increase in storage modulus, 70% improvement in hardness, and 40% enhancement in fracture toughness as compared to neat epoxy with the addition of only 0.5 wt% Ep-g-GO. In addition, the epoxy composites were thermally stable up to 300 °C. The improved dispersion of Ep-g-GO in the epoxy matrix led to a higher glass transition temperature of the composite, which can be attributed to the reduced macromolecular mobility of epoxy chains. Furthermore, this strategy was extended to epoxy/CF laminates. The addition of Ep-g-GO resulted in enhanced ultimate tensile strength, storage modulus, and ILSS by 12%, 24%, and 9%, respectively, as compared to neat epoxy/CF laminates. The laminates also showed improved flammability properties. The laminates showed up to −45 dB of EM radiation shielding, which makes them commercially useful for many applications. Thus, the present work demonstrates a significant improvement in the properties of epoxy composites and epoxy/CF laminates with the incorporation of 0.5 wt% Ep-g-GO due to better dispersion and improved interfacial adhesion.

Conflicts of interest

There are no conflicts to declare.

Acknowledgements

The authors would like to acknowledge the Aeronautics Research and Development Board (ARDB) (ARDB/01/2031796/M/I), India, for financial support. The authors would also like

to acknowledge AFMM, CeNSe, IISc, and NAL for providing various characterization facilities.

References

1 J. J. Chruściel and E. Leśniak, *Prog. Polym. Sci.*, 2015, **41**, 67–121.
2 Q. Ma, Y. Gu, M. Li, S. Wang and Z. Zhang, *Appl. Surf. Sci.*, 2016, **379**, 199–205.
3 E. Hammel, X. Tang, M. Trampert, T. Schmitt, K. Mauthner, A. Eder and P. Pötschke, *Carbon*, 2004, **42**, 1153–1158.
4 R. Rohini, P. Katti and S. Bose, *Polymer*, 2015, **70**, A17–A34.
5 B. Wetzel, P. Rosso, F. Haupert and K. Friedrich, *Eng. Fract. Mech.*, 2006, **73**, 2375–2398.
6 P. Katti, K. V. Kundan, S. Kumar and S. Bose, *ACS Omega*, 2018, **3**, 17487–17495.
7 D.-J. Kwon, P.-S. Shin, J.-H. Kim, Y.-M. Baek, H.-S. Park, K. L. DeVries and J.-M. Park, *Composites, Part B*, 2017, **130**, 46–53.
8 S. Jiang, Q. Li, J. Wang, Z. He, Y. Zhao and M. Kang, *Composites, Part A*, 2016, **87**, 1–9.
9 J. P. Johnston, B. Koo, N. Subramanian and A. Chattopadhyay, *Composites, Part B*, 2017, **111**, 27–36.
10 I. A. Ventura, A. Rahaman and G. Lubineau, *J. Appl. Polym. Sci.*, 2013, **130**, 2722–2733.
11 P. Katti, S. Bose and S. Kumar, *Polymer*, 2016, **102**, 43–53.
12 B. Francis, S. Thomas, G. V. Asari, R. Ramaswamy, S. Jose and V. L. Rao, *J. Polym. Sci., Part B: Polym. Phys.*, 2006, **44**, 541–556.
13 K. S. Novoselov, V. I. Fal′ko, L. Colombo, P. R. Gellert, M. G. Schwab and K. Kim, *Nature*, 2012, **490**, 192–200.
14 M. F. L. De Volder, S. H. Tawfick, R. H. Baughman and A. J. Hart, *Science*, 2013, **339**, 535–539.
15 J. Kim, L. J. Cote, F. Kim, W. Yuan, K. R. Shull and J. Huang, *J. Am. Chem. Soc.*, 2010, **132**, 8180–8186.
16 S.-Z. Zu and B.-H. Han, *J. Phys. Chem. C*, 2009, **113**, 13651–13657.
17 H. Bai, Y. Xu, L. Zhao, C. Li and G. Shi, *Chem. Commun.*, 2009, **13**, 1667–1669.
18 P. K. S. Mural, M. Sharma, G. Madras and S. Bose, *RSC Adv.*, 2015, **5**, 32078–32087.
19 P. Katti, K. Kundan, S. Kumar and S. Bose, *Polymer*, 2017, **122**, 184–193.
20 S. Liu, T. H. Zeng, M. Hofmann, E. Burcombe, J. Wei, R. Jiang, J. Kong and Y. Chen, *ACS Nano*, 2011, **5**, 6971–6980.
21 P. Xavier, K. Sharma, K. Elayaraja, K. Vasu, A. Sood and S. Bose, *RSC Adv.*, 2014, **4**, 12376–12387.
22 P.-G. Ren, D.-X. Yan, X. Ji, T. Chen and Z.-M. Li, *Nanotechnology*, 2011, **22**, 055705, 1–8.
23 P. K. S. Mural, A. Banerjee, M. S. Rana, A. Shukla, B. Padmanabhan, S. Bhadra, G. Madras and S. Bose, *J. Mater. Chem. A*, 2014, **2**, 17635–17648.
24 A. M. Díez-Pascual, G. Martínez, J. M. González-Domínguez, A. Ansón, M. T. Martínez and M. A. Gómez, *J. Mater. Chem.*, 2010, **20**, 8285–8296.
25 B. Shen, W. Zhai, M. Tao, D. Lu and W. Zheng, *Compos. Sci. Technol.*, 2013, **77**, 87–94.
26 Y.-J. Wan, L.-C. Tang, L.-X. Gong, D. Yan, Y.-B. Li, L.-B. Wu, J.-X. Jiang and G.-Q. Lai, *Carbon*, 2014, **69**, 467–480.
27 Y.-J. Wan, L.-X. Gong, L.-C. Tang, L.-B. Wu and J.-X. Jiang, *Composites, Part A*, 2014, **64**, 79–89.
28 M. G. Ahangari and A. Fereidoon, *Mater. Chem. Phys.*, 2015, **151**, 112–118.
29 M. Munz, *J. Phys. D: Appl. Phys.*, 2006, **39**, 4044.
30 R. Rohini and S. Bose, *Phys. Chem. Chem. Phys.*, 2015, **17**, 7907–7913.
31 T. Kuilla, S. Bhadra, D. Yao, N. H. Kim, S. Bose and J. H. Lee, *Prog. Polym. Sci.*, 2010, **35**, 1350–1375.
32 L. Chen, S. Chai, K. Liu, N. Ning, J. Gao, Q. Liu, F. Chen and Q. Fu, *ACS Appl. Mater. Interfaces*, 2012, **4**(8), 4398–4404.
33 X.-J. Shen, X.-Q. Pei, Y. Liu and S.-Y. Fu, *Composites, Part B*, 2014, **57**, 120–125.
34 M. Naebe, J. Wang, A. Amini, H. Khayyam, N. Hameed, L. H. Li, Y. Chen and B. Fox, *Sci. Rep.*, 2014, **4**, 4375, 1–7.
35 T. Walter, G. Subhash, B. Sankar, M. Song and C. Yen, *Exp. Mech.*, 2013, **53**, 493–503.
36 A. K. Pathak, M. Borah, A. Gupta, T. Yokozeki and S. R. Dhakate, *Compos. Sci. Technol.*, 2016, **135**, 28–38.
37 X. Zhang, X. Fan, C. Yan, H. Li, Y. Zhu, X. Li and L. Yu, *ACS Appl. Mater. Interfaces*, 2012, **4**, 1543–1552.
38 A. Petsom, S. Roengsumran, A. Ariyaphattanakul and P. Sangvanich, *Polym. Degrad. Stab.*, 2003, **80**, 17–22.
39 F. H. Gojny, M. H. Wichmann, B. Fiedler and K. Schulte, *Compos. Sci. Technol.*, 2005, **65**, 2300–2313.
40 J. Wang and Z. Han, *Polym. Adv. Technol.*, 2006, **17**, 335–340.
41 A. V. Menon, G. Madras and S. Bose, *Phys. Chem. Chem. Phys.*, 2017, **19**, 467–479.
42 S. Maya, S. Sukanya, A. Jiji, T. Sabu, M. Giridhar and S. Bose, *Mater. Res. Express*, 2014, **1**, 035003, 1–17.
43 S. Mishra, P. Katti, S. Kumar and S. Bose, *Chem. Eng. J.*, 2019, **357**, 384–394.
44 F. J. Baltá Calleja, R. K. Bayer and T. A. Ezquerra, *J. Mater. Sci.*, 1988, **23**, 1411–1415.